

See discussions, stats, and author profiles for this publication at: <https://www.researchgate.net/publication/309301055>

Fluorescence bio–barcode DNA assay based on gold and magnetic nanoparticles for detection of Exotoxin A gene sequence

Article in *Biosensors & Bioelectronics* · October 2016

DOI: 10.1016/j.bios.2016.10.030

CITATIONS

27

READS

256

4 authors, including:



Bahram Amini

17 PUBLICATIONS 198 CITATIONS

[SEE PROFILE](#)



Mehdi Kamali

Baqiyatallah University of Medical Sciences

29 PUBLICATIONS 410 CITATIONS

[SEE PROFILE](#)



Mojtaba Salouti

Islamic Azad University - Zanzan Branch

85 PUBLICATIONS 794 CITATIONS

[SEE PROFILE](#)

Some of the authors of this publication are also working on these related projects:



Isolation and rapid detection *Pseudomonas aeruginosa* by PCR [View project](#)



article [View project](#)



Fluorescence bio-barcode DNA assay based on gold and magnetic nanoparticles for detection of Exotoxin A gene sequence



Bahram Amini^a, Mehdi Kamali^{b,*}, Mojtaba Salouti^{c,*}, Parichehreh Yaghmaei^a

^a Department of Biology, Science and Research Branch, Islamic Azad University (IAU), Tehran, Iran

^b Nanobiotechnology Research Center, Baqiyatallah University of Medical Sciences, Tehran, Iran

^c Biology Research Center, Zanjan Branch, Islamic Azad University, Zanjan, Iran

ARTICLE INFO

Keywords:

Bio-barcode DNA
Gold nanoparticles
Exotoxin A
Pseudomonas aeruginosa

ABSTRACT

Bio-barcode DNA based on gold nanoparticle (bDNA-GNPs) as a new generation of biosensor based detection tools, holds promise for biological science studies. They are of enormous importance in the emergence of rapid and sensitive procedures for detecting toxins of microorganisms. Exotoxin A (ETA) is the most toxic virulence factor of *Pseudomonas aeruginosa*. ETA has ADP-ribosylation activity and decisively affects the protein synthesis of the host cells. In the present study, we developed a fluorescence bio-barcode technology to trace *P. aeruginosa* ETA. The GNPs were coated with the first target-specific DNA probe 1 (1pDNA) and bio-barcode DNA, which acted as a signal reporter. The magnetic nanoparticles (MNPs) were coated with the second target-specific DNA probe 2 (2pDNA) that was able to recognize the other end of the target DNA. After binding the nanoparticles with the target DNA, the following sandwich structure was formed: MNP 2pDNA/tDNA/1pDNA-GNP-bDNA. After isolating the sandwiches by a magnetic field, the DNAs of the probes which have been hybridized to their complementary DNA, GNPs and MNPs, via the hydrogen, electrostatic and covalently bonds, were released from the sandwiches after dissolving in dithiothreitol solution (DTT 0.8 M). This bio-barcode DNA with known DNA sequence was then detected by fluorescence spectrophotometry. The findings showed that the new method has the advantages of fast, high sensitivity (the detection limit was 1.2 ng/ml), good selectivity, and wide linear range of 5–200 ng/ml. The regression analysis also showed that there was a good linear relationship ($\Delta F = 0.57 [\text{target DNA}] + 21.31$, $R^2 = 0.9984$) between the fluorescent intensity and the target DNA concentration in the samples.

1. Introduction

Pseudomonas aeruginosa, a gram-negative obligate aerobe, is found in many natural and manmade environments. It has been isolated from plants, soils, water (Hanaki et al., 2010) and warm, moist environments containing very low levels of organic material. This organism is an opportunistic pathogen that infects humans and animals. In humans, *P. aeruginosa* is a common cause of nosocomial infections in burn and other immunocompromised patients including transplant, cancer and acquired immune deficiency syndrome patients (Hanaki et al., 2010). The numerous virulence factors of *P. aeruginosa* reflect its multifactorial pathogenicity and contribute to several infection stages. Surface factors including pili, lipopolysaccharides, and polysaccharide slime contribute to bacterial adherence and colonization. In contrast, different secreted proteins play a decisive role in

dissemination and tissue damage. *Pseudomonas* exotoxin A (ETA) is the most toxic substance in *P. aeruginosa*. Exotoxin A, produced by the most clinical strains of *P. aeruginosa*, is highly toxic for animals and tissue cultures. It belongs to a family of enzymes termed mono-ADP-ribosyltransferases, and inhibits protein synthesis *in vitro* and *in vivo* by enzymatic addition of adenosine 5-diphosphate ribose to elongation factor 2 (EF-2). Intake of trace amounts of ETA results in diarrhea, vomiting, septic shock and even death (Wolf and Beile, 2009).

Conventional analytical methods including radioimmunoassay, enzyme-linked immunosorbent assay (ELISA), fluorescence-based fiber optic immunoassay, aptamer microarrays, mass sensitive biosensor, microelectrochemical biosensors, electrochemiluminescent (ECL) (Zhang et al., 2012) quantitative polymerase chain reaction (PCR) assay (Melchior et al., 2010), amperometric immunosensor (Suresh et al., 2010), silica coating magnetic nanoparticle-based silver en-

Abbreviations: SMCC, sulfosuccinimidyl 4-Nmaleimidomethyl cyclohexane-1-carboxylate; APTES, 3-aminopropyltriethoxysilane; MNPs, magnetic nanoparticles; GNPs, gold nanoparticle; TEOS, tetraethoxysilane; DTT, dithiothreitol; ETA, exotoxin A; LB-broth, Luria Bertani broth

* Corresponding authors.

E-mail addresses: mehkamali@yahoo.co.uk (M. Kamali), saloutim@yahoo.com (M. Salouti).

<http://dx.doi.org/10.1016/j.bios.2016.10.030>

Received 27 June 2016; Received in revised form 10 October 2016; Accepted 18 October 2016

Available online 19 October 2016

0956-5663/ © 2016 Published by Elsevier B.V.

hancement immunoassay are effective for ETA detection (Zhang et al., 2010). Although these analytical methods are effective for ETA detection, but they are time consuming, difficult and expensive. Various PCR methods have been developed for nucleic acid detection in the past decade. Some common fluorescence probes such as fluorescent (Bi et al., 2006) metal ions (Zhang et al., 2013), metal complexes (Krishnamoorthy et al., 2011), nanoparticles (Zanoli et al., 2012), and bio-barcode DNA are the only bio-detection methods that have the PCR-like sensitivity for both protein and nucleic acid targets without any need for enzymatic amplification (Chang et al., 2007). Therefore, searching for new generations of fluorescent probes with especial properties to develop the DNA biosensors with lower detection limits, higher selectivity and very low background is of increasing interest. In this connection, the widespread use of nanomaterials has opened a new era in advancement of bio-analytical technology. Thus, the nanoparticles of metals and semiconductors with unique optical, electronic, magnetic and catalytic properties were introduced as potential candidates for use in optoelectronic nano devices, catalysts and nanobio-transducers (Li et al., 2013). In the past decade, gold nanoparticles (GNPs) have attracted an increasing attention in DNA sensors due to their easy preparation, good biocompatibility and unique optical properties (Saha et al., 2012). The easy modification of gold surface by thiol ended molecules makes it suitable for preparation of different biological assemblies, for using in chemosensing, bio sensing and immunosensing systems (Daniel et al., 2004). Compared to common genomic detection systems, the use of GNPs in DNA detection has increased the sensitivity up to ten-fold in some cases and improved the response characteristics (Kewal et al., 2005).

In the present project, two nanoparticles were utilized in the probes and barcode DNA design: amine-coated magnetic nanoparticles (probe 2-MNP) to separate the target DNA from the sample mixture, and probe1-capped GNPs (probe 1-GNP-barcode DNA) to label the separated target DNA by forming a sandwich structure (GNP-target DNA-MNP) and generating the signal. After conjugation of probes with nanoparticles and hybridization with the target DNA, a magnetic field was used to separate the sandwich complex consisting of GNP-target DNA-MNP. GNPs were used to increase the surface area for more binding amount of probes to target DNA. So in order to enhance the selective separation of target DNA (consequently enhancing the sensitivity), we performed the synthesis and use of amine functionalized iron oxide nanoparticles as highly sensitive affinity probes for detection of target DNA for the first time.

2. Experimental

2.1. Materials

Hydrogen tetrochloroaurate (III) trihydrate ($\text{HAuCl}_4 \cdot 3\text{H}_2\text{O}$) and sodium citrate dehydrate were purchased from Sigma (St. Louis, MO, USA). Dithiothreitol (DTT), Ethyl acetate, NaCl, Luria broth (LB-broth), Tetraethoxysilane (TEOS) and 3-aminopropyltriethoxysilane (APTES) were purchased from Merck, Germany. All oligonucleotides (probes and barcode DNA) were synthesized by Bioneer, Korea. Sulfo-succinimidyl 4-Nmaleimidomethyl cyclohexane-1-carboxylate (SMCC) and Sulfo-NHS acetate were purchased from Thermo (Pierce, Milwaukee, WI, USA). All solutions were prepared in distilled water. *Pseudomonas aeruginosa* ATCC27853.

2.2. Bacterial species

P. aeruginosa ATCC27853 (as a reference species) was purchased from Pasteur Institute, Tehran, Iran. Other species including *Staphylococcus aureus*, *Escherichia coli*, *Shigella dysenteriae* and *Vibrio cholerae* bacteria (as the negative controls) were isolated from clinical samples in Mousavi Hospital, Zanjan, Iran.

2.3. Bacterial DNA preparation

P. aeruginosa was grown on LB-broth for 12 h. Subsequently, 5 ml of the bacteria culture was centrifuged at 1400g for 5 min. Then, the chromosomal DNA was extracted using DNA purification kit (Roche Diagnostics GmbH, Mannheim, Germany High Pure PCR Template Preparation Kit). Genomic DNA was electrophoresed on 0.8% agarose gel, in order to check the quality of the purified product. The target DNA concentration was determined using a UV-vis spectrophotometer (Cary 4000, U.S) at 260 nm and it was stored at $-20\text{ }^\circ\text{C}$.

2.4. Probes and barcode DNA designing

The sequences of the thiol-capped oligonucleotides (Probe1 and prob2) and the barcode DNA were 5'-SH-CAACGACGCACTCAAGCTG-3', 5'-TTGGTTCGCTGAACCTGGCTG-SH-3' and 5'-TEXTTATTCGTAGCTAAAAA-SH-3' (Deng et al., 2010) respectively. In a BLAST search of Gen Bank DNA sequences (<http://www.ncbi.nlm.nih.gov/Genbank/index.html>), we found no homology with any known *P. aeruginosa* bacteria genes. The probe1, prob2 and the barcode DNA were synthesized by Bioneer Company, Korea.

2.5. Synthesis of GNPs

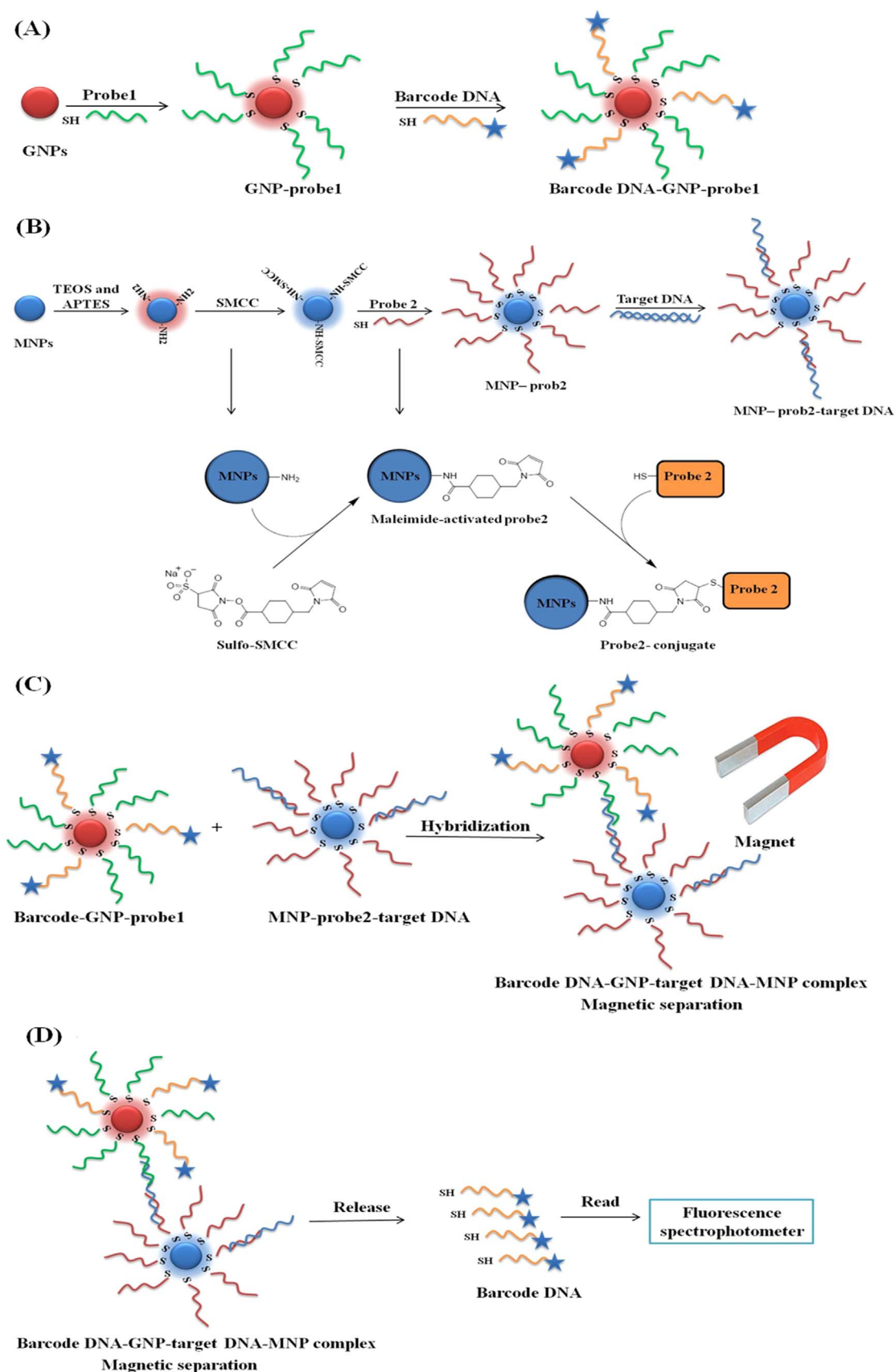
Colloidal GNPs of ~ 15 nm in diameter were synthesized by the citrate reduction method (Yangbao et al., 2015). Typically, 100 ml of HAuCl_4 (1 mM) solution was heated to reflux with vigorous stirring, then 10 ml of 38.8 mM sodium citrate was added to the mixture. The solution color changed from pale yellow to wine red within 1 min. The solution was heated under reflux for another 20 min. Then, the heating source was removed and the solution was continuously stirred until it cooled to room temperature ($25 \pm 2\text{ }^\circ\text{C}$). The resultant GNPs colloids were stored in $4\text{ }^\circ\text{C}$.

2.6. Synthesis of MNPs

Amino group modified silica coating of MNPs was performed using an improved Stober method which produces a relatively thick silica shell, as described by Zhang et al. (2010). 1.6 gr Fe_3O_4 and 0.8 gr Fe_2O_3 nanoparticles were mixed with 2.0 ml 2-propanol and 4.0 ml ethanol. 5.0 ml deionized water and 15 ml 25% (v/v) ammonia solution were added consecutively to the reaction mixture for 2 h at $80\text{ }^\circ\text{C}$. Under continuous mechanical stirring (rpm: 700), 10 ml 3-aminopropyltriethoxysilane (APTES) and 40 ml tetraethoxysilane (TEOS) were added to the reaction solution for 3 h at $80\text{ }^\circ\text{C}$. The hydrolysis and co-condensation of TEOS and APTES was initiated by adding of ammonia solution (25%) to the reaction mixture. The suspension of hybrid particles was separated by a magnetic field to remove all unreacted materials. The obtained pellet was redispersed in 10 ml water under sonication for 10 min. This purification step was repeated three times and the final suspensions were stored at $4\text{ }^\circ\text{C}$.

2.7. Mechanism of bio-barcode fluorescence

In the present study, a novel system based on bio-barcode fluorescence was developed for the detection of ETA gene. The sensing mechanism of the proposed MNP-target DNA-GNP bio-barcode for *P. aeruginosa* gene detection was shown in Scheme 1. We used MNPs for conjugation of probe 2 as a capture probe and GNPs for conjugation of the probe 1 and barcode DNA as the capture and reporter probes (Scheme 1A and B). Otherwise we had false positive response due to the release of barcode DNA from both free MNPs and those connected to the target DNA. This is because we have the probes and barcode DNA on the surface of all the MNPs and not just on the surface of MNPs connected to target DNA. The added target DNA of *P. aeruginosa* was co-hybridized with capture probes on GNPs and



Scheme 1. Schematic illustration of the bio-barcode assay; (A) formation of 1st DNA probe-GNP-barcode DNA complex; (B) formation of MNP-2nd DNA probe-target DNA complex; (C) formation of MNP-2nd DNA probe-target DNA-1st DNA probe-GNP-barcode DNA; (D) barcode DNA separation and release.

MNPs. After mixing the nanoparticles with the target DNA, the sandwich structure (MNP-2nd DNA probe/target DNA/1st DNA probe-GNP-barcode DNA) was formed (Scheme 1C). Then, the magnetic field was used to separate just the target DNA connected to the probes by the MNPs in the barcode DNA-GNP-probe 1-target DNA-probe 2-MNP complex. Next, the final mixture was washed to remove the free probes, free barcode DNA and free GNPs. After isolating the sandwiches by a magnetic field, the probes and barcode DNA hybridized to their complementary DNA bound on the GNPs and MNPs were released from the sandwich structure. The barcode DNA release of sandwich structure can be detected by fluorescence spectrophotometry (Scheme 1D).

2.8. Conjugation of GNPs

The thiol group of probes was unable to spontaneously form a layer on the surface of the nanoparticles. Therefore, in order to resolve the problem, the oligonucleotides (probe1 and barcode DNA) were dissolved in 100 μ l dithiothreitol solution (DTT 0.1 M, PBS 170 mM, pH 8) respectively for 2 h at room temperature until the disulfide bond was broken. Then, to remove DTT solution and to extract recovered oligonucleotides, 200 μ l ethyl acetate was added to the oligonucleotides. After stirring for 2 min, the upper phase liquid (organic) was separated from the lower phase liquid (water) by a sampler. This was repeated 3 times until the DTT was dissolved in organic phase and DTT was removed. The probe concentration was determined by Nano drop UV-Vis spectrophotometer after being extracted. The GNPs synthesized previously (1 ml), the purified thiolated barcode DNA (5 nmol), and the purified thiolated 1st DNA probe (0.05 nmol) were then mixed together. Thiolated DNA probe and barcode DNA would form a self-assembled monolayer on the surface of GNPs. Scheme 1A. showed a schematic illustration of the GNPs functionalization. After 16 h in the dark, the colloid solution was added to a 100 mM phosphate buffer (0.1 M PBS, pH 7.4) solution. The colloids were gradually added to 0.3 M NaCl by the dropwise addition of the 2 M NaCl solution. After a serial salt addition, the particles were stabilized for long-time storage at room temperature. Then the mixture was centrifuged at 4 °C. Following removal of the supernatant, the precipitate was washed with 0.3 M NaCl (pH 7.4) and 100 mM PBS solution, centrifuged and dispersed two times. After centrifugation, the colloid solution was suspended in (0.3 M NaCl pH 7 and 100 mM PBS) PBS solution at a final concentration of 10 nM and then it was stored at 4 °C (Deng et al., 2010).

2.9. Conjugation of MNPs

The MNPs synthesized previously and the polyamine-functionalized iron oxide particles (1 mg) were reacted with 300 μ g of sulfo-SMCC bio-functional linker for 2 h in 1 ml coupling buffer (0.1 M PBS buffer, 0.2 M NaCl, pH 7.4). The supernatant was removed after magnetic separation and the MNPs cross linker conjugate was rinsed with the coupling buffer three times. The reduced thiolated 2nd DNA probe (1 nmol) was added into 1 ml coupling buffer containing sulfo-SMCC modified MNPs and reacted for 8 h. Scheme 1B. showed the schematic illustration of the MNP-DNA probe2 conjugation. After conjugation, the DNA probe2 immobilized MNPs were rinsed with the coupling buffer three times. Then the functionalized MNPs were suspended in 35 ml of 10 mM sulfo-NHS acetate. The solution was incubated and shaken at room temperature to block the unreacted sulfo-SMCC on the surface of MNPs. After passivation, the particles were centrifuged at 4000 rpm for 5 min and washed with passivation buffer (0.2 M Tris, pH 8.5) and then with a storage buffer (100 mM PBS buffer, 0.2 M NaCl, pH 7.4) (Deng et al., 2010). The morphology and the size of the synthesized GNPs and MNPs were studied by transmission electron microscopy (TEM) and dynamic light scattering.

2.10. Target DNA detection

A solution containing target DNA in PCR tube was put in the thermo cycler at 95 °C for 10 min to separate the dsDNA into ssDNA. Serially diluted DNA samples (40 μ l) were mixed with 0.8 mg MNPs in 1000 μ l assay buffer (100 mM PBS buffer, 0.15 M NaCl, 0.1% SDS, pH 7.4). The hybridization reaction was maintained at a temperature of 50 °C for 40 min in an incubator. After hybridization, the MNPs with DNA target were washed twice with the assay buffer, and then suspended in 1000 μ l assay buffer (Scheme 1B and C). The functionalized GNPs (100 μ l) were centrifuged at 13,000 rpm for 20 min and the unreacted thiolated oligonucleotides in the supernatant were removed. Finally the purified GNPs complex was suspended in 500 μ l assay buffer. The GNPs complex (40 μ l) was then added into 200 μ l solution containing MNPs with target DNA. The hybridization was incubated at 50 °C for 2 h with shaking. After the sandwich structure (MNPs-2nd DNA probe-target DNA-1st DNA probe-GNP-barcode DNA) was formed, the sandwich structure was put on the magnetic separator for 3 min and then the supernatant was removed. The MNP-target DNA-GNP complex was washed three times with 500 μ l assay buffer and then stored at 4 °C.

2.11. Fluorescence measurements

The MNP-target DNA-GNP complex in different concentration of target DNA (5–200 ng/ml) was suspended in 200 μ l of 0.8 M DTT solution. In order to release the barcode DNA from the surface of GNPs, the MNP-target DNA-GNP complex was incubated at 65 °C for 45 min under vortex. After magnetic separation and centrifugation at 13,000 rpm for 20 min, the released barcode DNA was ready for fluorescent measurement (Scheme 1D). All fluorescence measurements were carried out an F-7000 fluorometer with excitation at 596 nm and emission at 613 nm for the barcode DNA fluorescence probes labeled by 5'-TEX613 as a fluorophore. The fluorescence intensity of the binding product and the blank were measured at the maximum wavelength. The fluorescence intensity of the binding product was recorded as F0 and F, in the absence and in the presence of ETA gene respectively. The change in fluorescence intensity ($\Delta F = \log F0 - F/F0$) was obtained by subtracting the fluorescence intensity of the binding product from that of the blank. ΔF and the concentration of ETA gene were used for quantitative detection of ETA gene. When the samples were excited 596 nm, the emission was scanned from 560 to 700 nm in steps of 1 nm and the scanning speed was 1200 nm/min (Deng et al., 2010).

3. Results and discussion

3.1. Characterization of GNPs and MNPs

Transmission electron microscopy and zeta seizer were used to study the morphology, size and potential distribution of the produce GNPs. Fig. 1A, B, G and H shown the TEM images of the GNPs before and after conjugation GNPs-probe1-target DNA complex. These results indicated that the GNPs have a well-defined spherical shape, potential -30 mV and an average dimension of 15 nm (Fig. 1A, G and H). Upon conjugation, the average diameter of GNPs conjugated probe of 23 nm was determined (Fig. 1B). This increase of 7–10 nm is consistent with the theoretical full layer coating with probe as the hydrodynamic diameter of a probe is approximately 6–8 nm. In addition, the shape and size of the MNPs were observed through transmission electron microscopy. The results showed that the MNPs were spherical and the diameter was ranging from 27 to 50 nm (Fig. 1C). Most of them (71%) were between 35 and 38 nm of size but after adding a probe to the surface of the nanoparticle, its size was increased to 45 nm (Fig. 1D).

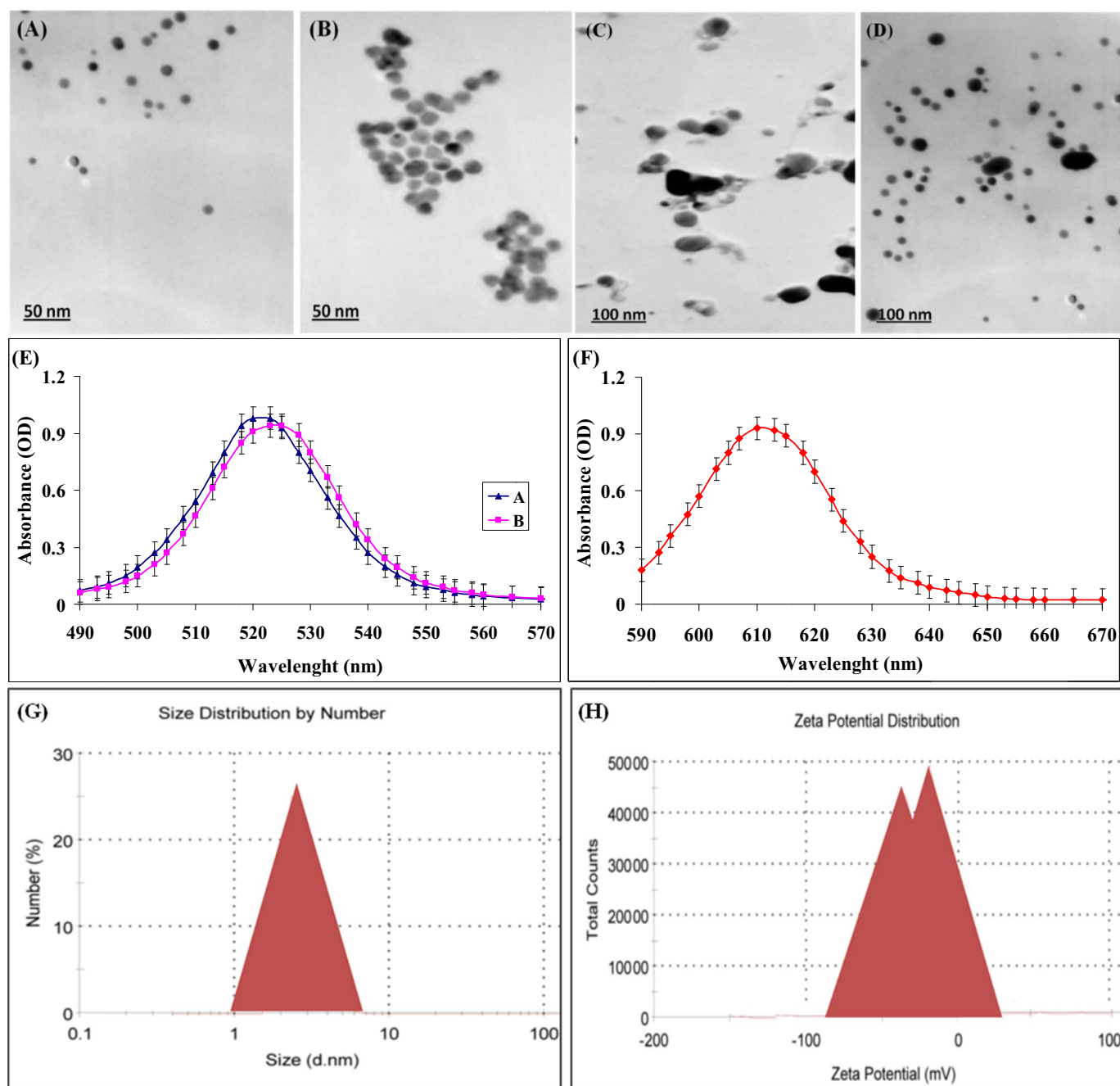


Fig. 1. TEM micrograph of synthesized GNPs and MNPs; (A) GNPs; (B) GNPs-probe-DNA; (C) MNPs; (D) barcode DNA-GNP-probe1-target DNA-probe2-MNP complex and UV-Vis spectra; (E, curve A) GNPs; (E, curve B) GNP-probes; (F) Barcode DNA-GNP-probe1-target DNA. (G and H) Analysis of size and potential distribution of the prepared GNPs measured by dynamic light scattering.

3.2. UV-Vis absorption spectra

The UV-Vis spectra of GNPs and probes DNA-functionalized GNPs in aqueous solutions are shown in Fig. 1E. There was a modest red-shift in the surface plasmon band from 520 to 525 nm after the DNA stabilization of the GNPs, which corroborated the limited aggregation in GNPs. It is well documented that GNPs can provide colorimetric contrast which is induced by surface plasmon resonance due to their quantum-size effect. Fig. 1E shows the absorption spectra of DNA-functionalized GNPs before (Fig. 1E, curve A) and after adding probes (Fig. 1E, curve B) and after hybridization with target DNA (Fig. 1F). As can be seen from Fig. 1E, curve A, GNPs showed a broad absorption band in the visible region around 520 nm. However, when a 10 ng/ml of target DNA was added, a modest red-shift in the surface plasmon

band from 520 to 610 nm was observed, due to the hybridization process, together with an increase in the absorbance between 600 and 700 nm. The absorbance peak was observed at 609 nm, the aggregation of GNPs found to turn the color of solution from red to blue.

3.3. Evaluation of conjugation efficiency

Fluorescence labeled barcode DNA was used to evaluate the conjugation efficiency. After the probes and the barcode DNA conjugated with GNPs, the probe-GNP-barcode DNA complex was suspended in 200 μ l of 0.8 M DTT solution. In order to release the barcode DNA from the surface of GNPs, the complex was incubated at 65 $^{\circ}$ C for 45 min under vortex. After separating GNPs by centrifugation at 13,000 rpm for 20 min the fluorescence signal of the supernatant

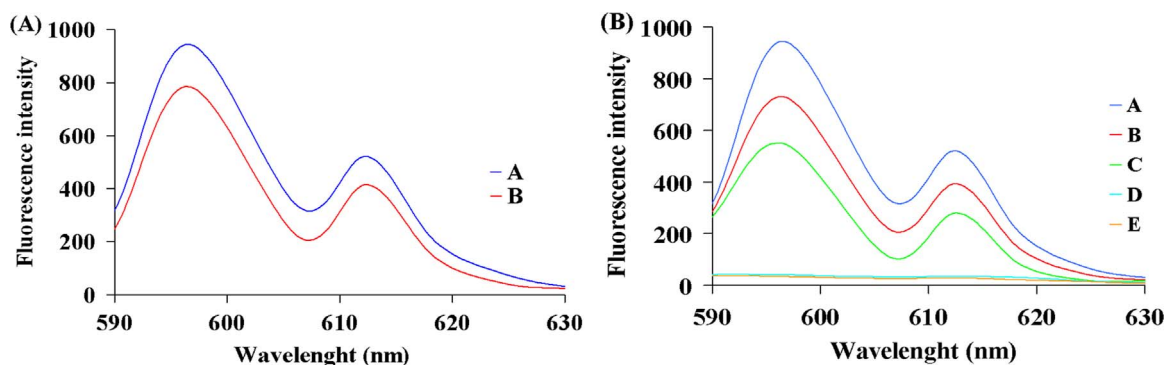


Fig. 2. Fluorescence spectrophotometric analysis; (A) showing the absorption peak of barcode DNA (TEX613; excitation=596 nm, emission=613 nm, (A; curve A)); fluorescence signal of supernatant solution for evaluation of conjugation efficiency (barcode DNA-GNP-probe1 complex) (A; curve B). (B) Absorption peak of free barcode DNA (B; curve A); barcode DNA released of probe1-GNP-barcode DNA complex (B; curve B); barcode DNA released of barcode DNA-GNP-probe1-target DNA-probe2-MNP complex (B; curve C); dsDNA (B; curve D) and ssDNA (B; curve E).

solution of 1st DNA probe/GNPs/barcode DNA-TEX 613 was measured (Fig. 2A).

3.4. Fluorescence spectra

In order to demonstrate the utility of the strategy, the fluorescence intensity changes from the interaction of the GNPs, MNPs and exotoxin A gene were investigated. We first investigated the fluorescence intensity of ds-DNA and ss-DNA templates. As shown in Fig. 2B, the fluorescence intensity was negligible when the two ss-DNA were used as the templates (Fig. 2B, curve D and E), respectively. However, an obvious fluorescence was obtained in the presence of 200 ng/ml ds-DNA templates (Fig. 2B, curve C). As can be seen from Fig. 2B, for the barcode DNA without nanoparticles (Fig. 2B, curve A), the formed barcode DNA-GNP-probe1 exhibited excellent fluorescence at 613 nm (Fig. 2B, curve B). However, the fluorescence of barcode DNA-GNP-probe1 was quenched greatly upon adding exotoxin A gene to the barcode DNA-GNP-probe1 solution. In order to resolve this problem, we released barcode DNA of GNP-barcode DNA complex and GNP-barcode DNA-target DNA-MNP complex. The result is shown in Fig. 2B, curve B and C. The results showed that the barcode DNA released of the surface GNPs could serve as a highly efficient fluorescent barcode DNA to detect exotoxin A gene.

3.5. Effect of temperature on hybridization

The effect of temperature on fluorescence intensity of the probe-functionalized GNPs and MNPs in the presence of target DNA at pH 7.4 and hybridization time of 45 min was studied and the results are shown in Fig. 3A. The temperatures were tested 20–60 °C. The maximum change in fluorescence intensity occurred at 50 °C. This may cause hybridization of the target DNA by the probes. As seen, the extent of fluorescence intensity is increased with increasing temperature due to the dehybridization of the target DNA. The melting temperature (T_m) for the DNA hybridization, defined as the temperature where 50% of the initial fluorescence intensity is observed, was approximated as about 45 °C.

3.6. Effect of time on hybridization

Fig. 3B showed the influence of time in the detection. The fluorescence intensity of the system increased gradually with an increase in the reaction time. Target DNA combined with GNPs and MNPs through the DNA-probes interaction. When the incubation time was over 45 min, there was no obvious increase in fluorescence intensity, which means the reaction reached a state of equilibrium. When the incubation time was from 40 to 80 min, the fluorescence intensity kept stable. Therefore, 45–80 min was chosen as the experi-

mental condition in this study.

3.7. Effect of PBS concentration on the hybridization

The effect of concentrations of PBS buffer saline during the detection was shown in Fig. 3C. It was found that with the increasing concentration of PBS buffer saline, the change of fluorescence intensity between binding product and the blank showed a trend of rise first then fall. The maximum change in fluorescence intensity occurred at 100 mM/l. This may have been due to the fact that the reaction between ETA gene and probes needs certain ionic strength. When the concentration of PBS is low, the ETA could not react well with probe1-GNP and probe2-MNP. Thus, the concentration of 100 mM/l was selected in this study.

3.8. Effect of pH on the hybridization

pH of buffer solution was investigated in this study. The results showed that the most suitable pH is 7.4. The reason might be that pH of Tris buffer solution influenced the effect of DNA hybridization among the capture probes DNA, target DNA and barcode DNA. In slightly alkaline solution, the effect of DNA hybridization should be better. Therefore, pH 7.4 was used for the following experiments (Fig. 3D).

3.9. Sensitivity

According to the above procedures, the calibration curve for target DNA determination was constructed under the optimal conditions. The fluorescence spectra of barcode DNAs released from the complex, MNP-probe2-target DNA-probe1-GNP-barcode DNA, in different concentrations of target DNA were shown in Fig. 4A. With increasing concentrations of target DNA (from 5 to 200 ng/ml), the fluorescence intensity of the complex was enhanced proportionately, because the target DNA can be conjugated by barcode DNA-GNP-probe1 and MNP-probe2. After connecting barcode DNA to GNP-probe1-target DNA-probe2-MNP complex, the fluorescence intensity was reduced in different concentration of target DNA. In order to resolve the problem, barcode DNA-GNP-probe1-target DNA-probe2-MNP complex in different concentrations of target DNA was suspended in 200 μ l of 0.8 M DTT solution to release the barcode DNA from the surface of GNPs. After the barcode DNA release by fluorescence spectrophotometry, fluorescence intensity was measured. The results showed that the fluorescence intensity of the system was increased in different concentration of ETA (Fig. 4A). In this way, we established the bio-barcode-fluorescence analysis method for ETA detection.

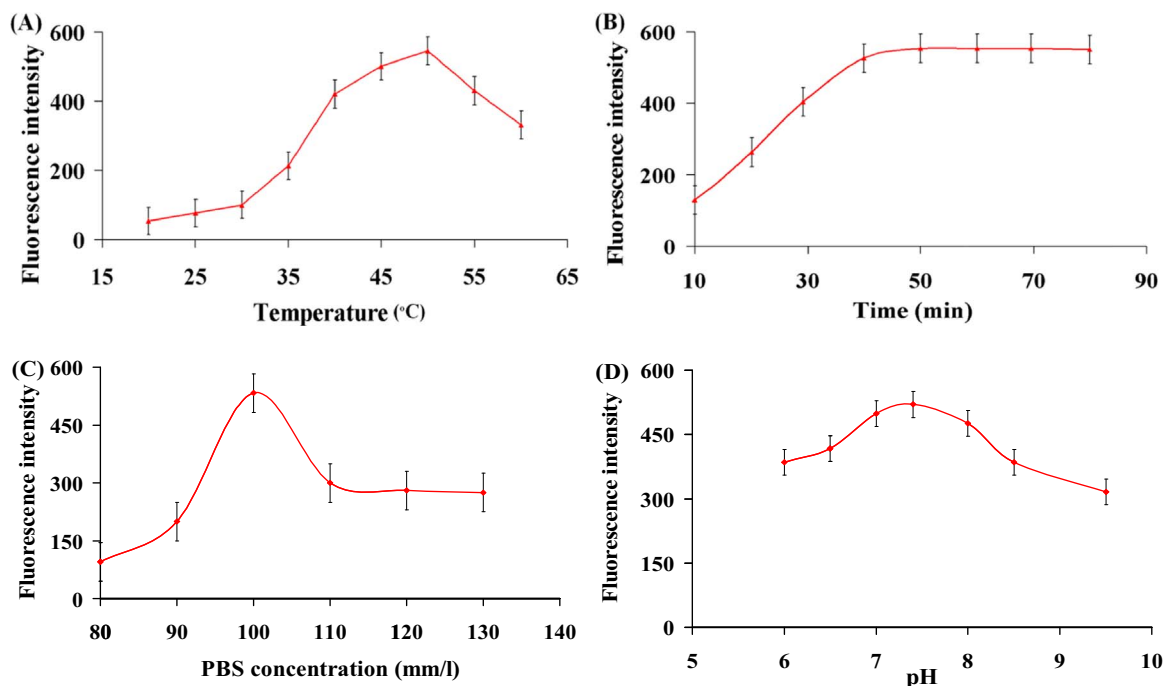


Fig. 3. (A) Effect of temperature on the conjugation system; at 200 ng/ml target DNA. The incubation temperature was 20, 25, 30, 35, 40, 45, 50, 55 and 60 °C; (B) effect of the time on fluorescence intensity. The incubation time was 10, 20, 30, 40, 50, 60, 70, and 80 min; (C) effect of concentration of PBS on the conjugation; the changed concentration of target DNA (at 200 ng/ml target DNA); (D) effect of pH on the conjugation; ETA gene concentration: at 200 ng/ml target DNA.

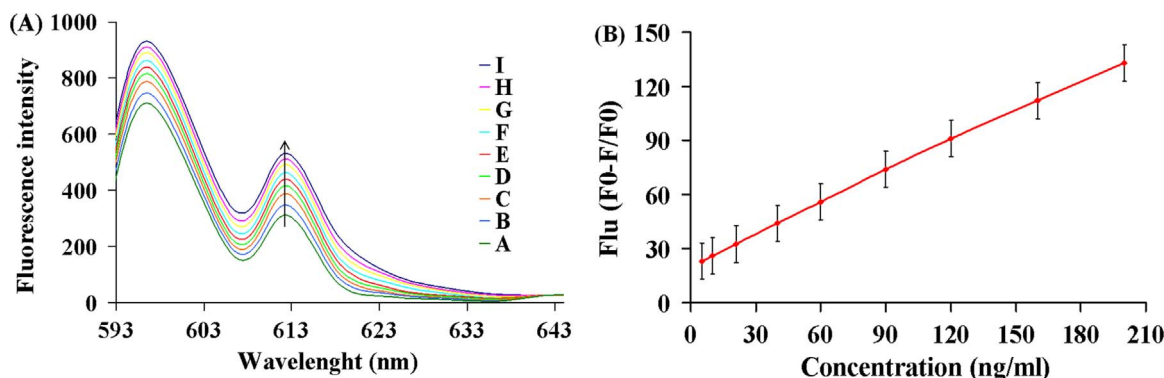


Fig. 4. (A) Changes in fluorescence spectra in the presence of different concentrations of target DNA. Concentrations of target DNA from (a) to (I): 5, 10, 20, 40, 60, 90, 120, 160 and 200 ng/ml, $\lambda=613$ nm; (B) liner relationships between concentrations of target DNA and changes in fluorescence intensity. Concentrations target DNA is 5, 10, 20, 40, 60, 90, 120, 160 and 200 ng/ml.

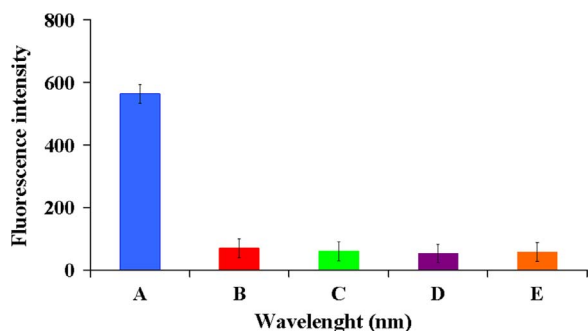


Fig. 5. Selectivity evaluation of the proposed probes and barcode DNA for the detection of target DNA. (A) *P. aeruginosa* at 200 ng/ml, (B) *Staphylococcus aureus*, (C) *Escherichia coli*, (D) *Shigella dysentery*, (E) *Vibrio cholera*. The concentrations of controls were 200 ng/ml.

3.10. The detection range and limit of detection

Under optimal conditions, the fluorescence intensity of the system

Table 1

The recovery and RSD value of detecting target DNA (ETA).

Number of sample	Amount added (ng/ml)	Amount found (ng/ml)	Recovery (%)	RSD (%)
1	3.0	2.95	98.3	1.1
2	5.0	5.1	102	1.06
3	7.5	7.4	98.7	1.14
4	10.0	10.18	101.8	1.03

with different concentrations of ETA gene was measured, and the calibration curve was constructed according to the relationship between the target DNA concentration and the corresponding fluorescence intensity change (ΔF). Fig. 4B illustrates the linear increase in the fluorescence intensity with increased concentration of ETA gene. The linear range for ETA gene was from 5 to 200 ng/ml and standard regression equation was $\Delta F=0.57$ [target DNA]+21.31, with the correlation coefficient $R^2=0.9984$. The limit of detection (LOD) refers to three times the value of the instruments background signal produced by the matrix blank. It indicates the sensitivity of the methods and

instruments. It is defined by the equation $LOD=3S_0/K$, where S_0 is the standard deviation of blank measurements ($n=8$) and K is the slope of the calibration graph. Here, the LOD was 1.2 ng/ml.

3.11. Specificity

The specificity of the fluorescent barcode DNA and probes was further inspected by exposing the target DNA to five kinds of bacteria, including *P. aeruginosa*, *Staphylococcus aureus*, *Escherichia coli*, *Shigella dysenteriae* and *Vibrio cholera* at the same concentration of 200 ng/ml. As shown in Fig. 5, there was no significant fluorescence increase upon the addition of above bacteria except viable *P. aeruginosa*. This high specificity to target DNA *P. aeruginosa* might be attributed to the high affinity and good selectivity of the probes against viable *P. aeruginosa*. So, these results indicated that the good specificity of the probes is suitable for detecting the *P. aeruginosa* indirectly.

3.12. Analysis of real samples

To further test the accuracy of this method, recoveries of target DNA from the clinical samples was analyzed and the results was indicated in Table 1. We determined target DNA in four groups, and each group was determined with three replicates. The target DNA concentrations are shown in Table 1. The obtained recoveries were in the range of 98.3–102%. These results indicate that the proposed method is highly accurate and reproducible for rapid detection of ETA in clinical samples.

4. Conclusion

In summary, a new fluorescence method for detecting ETA gene based on nanoparticles has two nanoparticles: GNPs and MNPs. The

GNPs work as signal reporter and the MNPs act as separator. The conjugation reaction between the two nanoparticles and thiolated oligonucleotides was efficient. After mixing the nanoparticles with the target DNA, the sandwich structure (MNPs-2nd DNA probe-target DNA-1st DNA probe-GNPs-barcode DNA) was formed. The fluorescence signal of released barcode DNA had a linear relationship with target DNA concentration. Results showed that under the optimum conditions, this method allowed the selective detection of ETA gene clinical specimens with the detection limit of 1.2 ng/ml. It had a high sensitivity, a good specificity, and a wide linear range (5–200 ng/ml). Regression analysis showed that there is a good linear relationship ($\Delta F=0.57 [\text{target DNA}] + 21.31$, $R^2=0.9984$) between fluorescent intensity and target DNA concentration in the sample. In particular, this is the first time that fluorescence sensor between MNPs and GNPs was used for the detection of ETA gene.

References

- Bi, S., Qiao, C., Song, D., et al., 2006. *Sens. Actuators B* 119, 199–208.
- Chang, T.L., Tsai, C.Y., Sun, C.C., et al., 2007. *Biosens. Bioelectron.* 22, 3139–3145.
- Daniel, M.C., Astruc, D., 2004. *Chem. Rev.* 104, 293–346.
- Deng, Z.M.C., Huarng, E.C.A., 2010. *Biosens. Bioelectron.* 26, 1736–1742.
- Hanaki, K.I., Goto, M., Shimada, K., et al., 2010. *J. Microbiol. Methods* 81, 247–252.
- Kewal, K., Jain, T., 2005. *Clin. Chim. Acta* 358, 37–54.
- Krishnamoorthy, P., Sathyadevi, P., Cowley, A.H., et al., 2011. *Eur. J. Med. Chem.* 46, 376–387.
- Li, X., Antonietti, M., 2013. *Chem. Soc. Rev.* 42, 6593–6604.
- Melchior, J.W.B., Tolleson, W.H., 2010. *Anal. Biochem.* 396, 204–211.
- Saha, K., Agasti, S.S., Kim, C., 2012. *Chem. Rev.* 112, 2739–2779.
- Suresh, S., Gupta, A.K., Rao, V.K., et al., 2010. *Talanta* 81, 703–708.
- Wolf, P., Beile, U.E., 2009. *Int. J. Med. Microbiol.* 299, 161–176.
- Yangbao, M.N.G., Tianhua, L.H.Z., Yuting, C.Q.J., 2015. *Sens. Actuators B* 220, 679–687.
- Zanoli, L.M., Agata, R.D., Spoto, G., 2012. *Anal. Bioanal. Chem.* 402, 1759–1771.
- Zhang, J., Cheng, T., Gao, L.Z., et al., 2010. *Toxicol.* 55, 145–152.
- Zhang, J., Wang, S., Yang, S., et al., 2012. *Toxicol.* 59, 12–16.
- Zhang, Y., Zhao, H., Wu, Z., et al., 2013. *Biosens. Bioelectron.* 48, 180–187.